

# Neutron guide optimisation for a time-of-flight neutron imaging instrument at the European Spallation Source

A. Hilger,<sup>1,\*</sup> N. Kardjilov,<sup>1</sup> I. Manke,<sup>1</sup> C. Zender,<sup>1,2</sup> K. Lieutenant,<sup>1</sup> K. Habicht,<sup>1</sup>  
J. Banhart,<sup>1</sup> and M. Strobl<sup>2</sup>

<sup>1</sup>Helmholtz-Zentrum Berlin, 14109 Berlin, Germany

<sup>2</sup>European Spallation Source AB, Lund, Sweden

\*hilger@helmholtz-berlin.de

**Abstract:** A neutron transport system for the planned imaging instrument ODIN at the future European Spallation Source (ESS) based on neutron optical components was designed and optimized. Different ways of prompt pulse suppression were studied. The spectral performance of the optimal neutron guide configuration is presented. In addition, the influence of the gaps in the guide system needed for the required chopper configuration was investigated. Given that the requirements for an imaging instrument located on a long guide system and hosting a complex chopper system are extremely demanding in terms of spectral and divergence needs, this study can be beneficial for a wide range of instruments in various ways.

©2015 Optical Society of America

**OCIS codes:** (110.0110) Imaging systems; (120.4570) Optical design of instruments; (230.7370) Waveguides; (080.4035) Mirror system design; (110.6960) Particles; (110.6960) Tomography.

---

## References and links

1. M. Strobl, "Future prospects of imaging at spallation neutron sources," *Nucl. Instrum. Meth. A* **604**(3), 646–652 (2009).
2. N. Kardjilov, I. Manke, A. Hilger, M. Strobl, and J. Banhart, "Neutron imaging in materials science," *Mater. Today* **14**(6), 248–256 (2011).
3. M. Strobl, I. Manke, N. Kardjilov, A. Hilger, M. Dawson, and J. Banhart, "Advances in neutron radiography and tomography," *J. Phys. D Appl. Phys.* **42**(24), 243001 (2009).
4. J. Banhart, *Advanced Tomographic Methods in Materials Research and Engineering* (Oxford University Press, Oxford, UK, 2008).
5. J. Banhart, A. Borbely, K. Dzieciol, F. Garcia-Moreno, I. Manke, N. Kardjilov, A. R. Kysser-Pyzalla, M. Strobl, and W. Treimer, "X-ray and neutron imaging – Complimentary techniques for materials science and engineering," *Int. J. Mater. Res.* **101**(9), 1069–1079 (2010).
6. N. Kardjilov, I. Manke, M. Strobl, A. Hilger, W. Treimer, M. Meissner, T. Kris, and J. Banhart, "Three-dimensional imaging of magnetic fields with polarized neutrons," *Nat. Phys.* **4**(5), 399–403 (2008).
7. M. Dawson, I. Manke, N. Kardjilov, A. Hilger, M. Strobl, and J. Banhart, "Imaging with polarized neutrons," *New J. Phys.* **11**(4), 043013 (2009).
8. M. Schulz, P. Schmakat, C. Franz, A. Neubauer, E. Calzada, B. Schillinger, P. Böni, and C. Pfeleiderer, "Neutron depolarisation imaging: Stress measurements by magnetostriction effects in Ni foils," *Physica B* **406**(12), 2412–2414 (2011).
9. I. Manke, N. Kardjilov, M. Strobl, A. Hilger, and J. Banhart, "Investigation of the skin effect in the bulk of electrical conductors with spin-polarized neutron radiography," *J. Appl. Phys.* **104**(7), 076109 (2008).
10. M. Strobl, C. Pappas, A. Hilger, S. Wrlert, N. Kardjilov, S. O. Seidel, and I. Manke, "Polarized neutron imaging: A spin-echo approach," *Physica B* **406**(12), 2415–2418 (2011).
11. M. Strobl, C. Grünzweig, A. Hilger, I. Manke, N. Kardjilov, C. David, and F. Pfeiffer, "Neutron dark-field tomography," *Phys. Rev. Lett.* **101**(12), 123902 (2008).
12. C. Grünzweig, C. David, O. Bunk, M. Dierolf, G. Frei, G. Kühne, J. Kohlbrecher, R. Schäfer, P. Lejcek, H. M. Rønnow, and F. Pfeiffer, "Neutron decoherence imaging for visualizing bulk magnetic domain structures," *Phys. Rev. Lett.* **101**(2), 025504 (2008).
13. I. Manke, N. Kardjilov, R. Schäfer, A. Hilger, M. Strobl, M. Dawson, C. Grünzweig, G. Behr, M. Hentschel, C. David, A. Kupsch, A. Lange, and J. Banhart, "Three-dimensional imaging of magnetic domains," *Nat. Commun.* **1**(8), 125 (2010).

14. A. Hilger, N. Kardjilov, T. Kandemir, I. Manke, J. Banhart, D. Penumadu, A. Manescu, and M. Strobl, "Revealing microstructural inhomogeneities with dark-field neutron imaging," *J. Appl. Phys.* **107**(3), 036101 (2010).
15. S. W. Lee, K. Y. Kim, O. Y. Kwon, N. Kardjilov, M. Dawson, A. Hilger, and I. Manke, "Observation of magnetic domains in insulation-coated electrical steels by neutron dark-field imaging," *Appl. Phys. Express* **3**(10), 106602 (2010).
16. J. R. Santisteban, L. Edwards, A. Steuwer, and P. J. Withers, "Time-of-flight neutron transmission diffraction," *J. Appl. Cryst.* **34**(3), 289–297 (2001).
17. M. Strobl, N. Kardjilov, A. Hilger, D. Penumadu, and I. Manke, "Advanced neutron imaging methods with a potential to benefit from pulsed sources," *Nucl. Instrum. Meth. A* **651**(1), 57–61 (2011).
18. M. Strobl, R. Woracek, N. Kardjilov, A. Hilger, R. Wimpory, A. Tremsin, T. Wilpert, C. Shulz, I. Manke, and D. Penumadu, "Time-of-flight neutron imaging for spatially resolved strain investigations based on Bragg edge transmission at a reactor source," *Nucl. Instrum. Meth. A* **680**, 27–34 (2012).
19. N. Kardjilov, A. Hilger, I. Manke, M. Strobl, S. Williams, M. Dawson, and J. Banhart, "Neutron tomography instrument CONRAD at HZB," *Nucl. Instrum. Meth. A* **651**(1), 47–52 (2011).
20. W. Kockelmann, G. Frei, E. H. Lehmann, P. Vontobel, and J. R. Santisteban, "Energy-selective neutron transmission imaging at a pulsed source," *Nucl. Instrum. Meth. A* **578**(2), 421–434 (2007).
21. A. S. Tremsin, J. B. McPhate, W. Kockelmann, J. V. Vallerger, O. H. W. Siegmund, and W. B. Feller, "High-resolution Bragg edge transmission spectroscopy at pulsed neutron sources: Proof of principle experiments with a neutron counting MCP detector," *Nucl. Instrum. Meth. A* **633**, S235–S238 (2011).
22. W. Treimer, M. Strobl, N. Kardjilov, A. Hilger, and I. Manke, "Wavelength tunable device for neutron radiography and tomography," *Appl. Phys. Lett.* **89**(20), 203504 (2006).
23. R. Woracek, D. Penumadu, N. Kardjilov, A. Hilger, M. Strobl, R. Wimpory, I. Manke, and J. Banhart, "Neutron based Bragg-edge radiography and strain mapping under in-situ tensile loading," *J. Appl. Phys.* **109**, 093506 (2011).
24. E. H. Lehmann, G. Frei, P. Vontobel, L. Josic, N. Kardjilov, A. Hilger, W. Kockelmann, and A. Steuwer, "The energy-selective option in neutron imaging," *Nucl. Instrum. Meth. A* **603**(3), 429–438 (2009).
25. N. Kardjilov, I. Manke, A. Hilger, S. Williams, M. Strobl, R. Woracek, M. Boin, E. Lehmann, D. Penumadu, and J. Banhart, "Neutron Bragg-edge mapping of weld seams," *Int. J. Mater. Res.* **103**(02), 151–154 (2012).
26. K. Lefmann, K. Nielsen, A. Tennant, and B. Lake, "McStas 1.1: a tool for building neutron Monte Carlo simulations," *Physica B* **276–278**, 152–153 (2000).
27. D. Wechsler, G. Zsigmond, F. Streffer, and F. Mezei, "VITESS: Virtual instrumentation tool for pulsed and continuous sources," *Neutron News* **11**(4), 25–28 (2000).
28. M. Strobl, M. Bulat, and K. Habicht, "The wavelength frame multiplication chopper system for an ESS test-beamline and corresponding implications for ESS instruments," *Nucl. Instrum. Meth. A* **705**, 74–84 (2013).
29. ESS Technical Design Report: <http://eval.ess.lu.se/cgi-bin/public/DocDB/ShowDocument?docid=274>
30. C. Zendeler, K. Lieutenant, D. Nekrassov, L. D. Cussen, and M. Strobl, "Bi-spectral beam extraction in combination with a focusing feeder," *Nucl. Instrum. Meth. A* **704**, 68–75 (2013).

## 1. Introduction

The new generation of powerful pulsed spallation neutron sources not only promotes neutron scattering instrumentation in general but also enables novel neutron imaging techniques and associated beam lines [1]. Since recent developments of neutron imaging methods [1–5] include approaches that benefit from or are enabled by wavelength resolution [5–14], neutron imaging can take significant advantage of pulsed sources [1,15–17]. In contrast to many state-of-the-art imaging instruments at continuous sources [18] such instruments require, dependent on the time structure of the pulsed source, a certain length in order to obtain the desired wavelength resolution for time-of-flight (TOF) imaging methods [1,15,17–25]. As the planned European Spallation Source (ESS) will be a long-pulse source, instruments at the ESS will typically require longer neutron guide systems than elsewhere. Due to an envisaged moderator-to-detector length of about 60 m, the planned imaging instrument ODIN at ESS will need a dedicated neutron guide system. The selected pulse shaping and wavelength-frame-multiplication (WFM) chopper system will allow for taking full advantage of the flexibility of the long-pulse to tune the TOF resolution to the needs of specific measurements but will also imply some limitations and requirements to the guide system. Special attention has to be paid to the suppression of prompt pulse contamination of the beam and to the provision of a spatially and spectral homogeneous beam over the field of view (FOV) of the imaging detector.

We report how, after the boundary conditions and desired parameters have been defined for the instrument, a number of potential solutions have been examined and optimized by means of ray tracing simulations utilizing the program packages McSTAS [26] and VITESS [27].

## **2. Basic considerations. Boundary conditions and desired instrument parameters (benchmarks)**

The baseline design of the long-pulse neutron source ESS defines the source to be operated at a repetition rate of 14 Hz and a pulse length of 2.86 ms. In order to reach the coarsest desired wavelength resolution of 10% for 2-Å neutrons while using the full pulse of 2.86 ms, a length of 60 m is considered for the instrument. The instrument will be based on a pinhole geometry, with the pinhole placed 50 m from the source in order to allow for a proper collimation on a large FOV at the detector position at 60 m distance, see Fig. 1(a). The design aims at a FOV of  $250 \times 250 \text{ mm}^2$ . Consequently, the priority of the guide system to be developed lies on the transport of a high flux density of all required wavelengths with a homogeneous and sufficient divergence to the pinhole at the 50 m position in order to illuminate the FOV plane evenly. For the simulations, the maximum pinhole diameter was set to 30 mm. This corresponds to a collimation ratio  $L/D$  of 333, where  $L$  denotes the pinhole-to-detector distance (10 m) and  $D$  the pinhole diameter. This collimation ratio is a reasonable mean value that can be tuned for specific measurements and spatial resolution requirements by varying either  $L$  or  $D$ .

Some boundary conditions have to be taken into account. For reasons of efficiency and flexibility, a pair of pulse shaping choppers will be placed at around 6 m from the moderator, right outside the source-shielding monolith. In order to achieve the required accuracy of beam chopping also for high TOF resolutions, for example as required for strain mapping by measuring the Bragg edges in the transmitted signal, the beam size has to be limited in this position to  $15 \times 15 \text{ mm}^2$ , see Fig. 1(a). Although chopping would require such limitation only in one direction a symmetric solution was initially chosen in favour of the beam homogeneity on the FOV. In addition, these choppers have to be movable along the beam within a range of 0.5 m in order to allow the tuning and tailoring of the wavelength resolution to the requirements of the measurement [28]. This requires a corresponding gap in the guide system from about 6 m to 6.5 m from the moderator. As the full WFM chopper system also requires a number of frame overlap choppers along the guide, the maximum cross section of the guide has been limited to  $100 \times 100 \text{ mm}^2$ .

It is well known from existing imaging facilities located at neutron guides (CONRAD-2 at HZB [19] and the imaging beam lines at Saclay and HFIR) that any discontinuity or inhomogeneity in the divergence distribution introduced by reflections in the guide system and especially also by guide joints, which are required, e.g., for the choppers, give rise to corresponding line patterns, characterized by associated minima, in the intensity distribution on the FOV. These patterns become more distinct when the  $L/D$  ratio is increased e.g. by decreasing the pinhole size. However, the experience in neutron imaging involving neutron guide systems have proven that smooth variations with correspondingly moderate intensity variations do not impact on the quality of measurements as they can be corrected straightforwardly just as efficiency variations over the detector surface. A quality threshold of 10% variation in a central plateau area of  $200 \times 200 \text{ mm}^2$  has been defined. The line pattern problem can be overcome using a thin graphite powder diffuser as has been recently demonstrated at the new CONRAD-2 facility at HZB. However, this sacrifices some moderate flux density for improved homogeneity.

Finally, in order to benchmark the quality and efficiency of the guide system for imaging, simulations of the most straight-forward imaging set-up at a neutron source, involving only a pinhole at the 6.25 m position and the corresponding FOV at 16.25 m have been carried out, Fig. 1(ai). In this way the efficiency of the guide system which is transporting the neutron intensity to the pinhole can be studied.

Taking into account these boundary conditions the basic approach to the guide system was to extract the beam by a feeder between 2 m and 6 m from the moderator. The feeder focuses the beam between the pulse shaping choppers at about 6.25 m distance where a square slit of  $15 \times 15 \text{ mm}^2$  area is placed. The role of the slit is to reduce the “smearing” of the pulse produced from the chopper and in this way to increase the wavelength resolution of the instrument. From this “virtual source” the beam enters into a diverging guide section and changes to a nearly constant cross section in a middle part, before refocussing at 50 m distance from the moderator at the location of the pinhole. The aim is to obtain the best possible transport of the beam from the first slit to the pinhole.

### 3. Guide optimisation

The feeder was first optimized independently and an optimum with respect to intensity was found for a 4-m long parabolic section with an entrance window of  $75 \times 75 \text{ mm}^2$  at 2 m distance from the  $120 \times 120 \text{ mm}^2$  large moderator surface (ESS TDR [29] baseline). The section is tapered parabolically towards a  $19.72 \times 19.72 \text{ mm}^2$  cross section at 6 m and has a focal spot at 6.297 m distance. For this optimization, the size of the entrance window and the position of the entrance focal point were varied in small steps until maximum intensity at the focal spot was achieved. After that, the parameters were tuned until a homogenous beam distribution at the detector position at 60 m was obtained, while using different downstream guide systems presented below.

For the downstream guide system starting at 6.5 m distance from the moderator, different geometries have been investigated and optimized. These approaches include a continuous elliptic guide with focal spots close to the slit position at 6.25 m as well as in the pinhole at 50 m distance, see Fig. 1(aii), a solution with elliptic entrance and exit sections connected by a long straight section in the middle, see Fig. 1(aiii), and a similar solution with parabolic tapered start and end sections, see Fig. 1(aiv). Besides the limitation in maximum cross section, the parameters kept fixed throughout optimization were: the cold moderator used; the supermirror coating with  $m = 5$  (which allows for reflection of neutrons with 5 times the divergence than by a mirror based on a single Ni layer); the symmetric rectangular cross section; the position of the pinhole and the FOV position at 60 m.

A comparison of the numerical optimization through simulations of the benchmark (i) and the three options (ii,iii,iv) is given in Fig. 1(b). Clearly the continuous elliptic solution (ii) provides the best intensity transfer, however with a distinct decrease above a certain divergence resulting in a significant flux density drop outside a central area of  $70 \times 70 \text{ mm}^2$  of the FOV. The reason for this is the contribution of the single reflected neutrons from the elliptical mirrors which are building up the shape of the moderator through the pinhole arrangement on the FOV plane. The intensity transfer for the elliptic and parabolic tapered guides (iii, iv) is lower but especially (iii) gives rise to a significantly more homogeneous beam within the FOV due to the middle straight section where the neutrons undergo multiple reflections. The loss in intensity as compared to the benchmark is characterized by an overall factor of about two. The resulting parameters for all the configurations are provided in Table 1. Note that the relative losses as compared to the benchmark can be partially regained by the foreseen bi-spectral extraction described in [30].

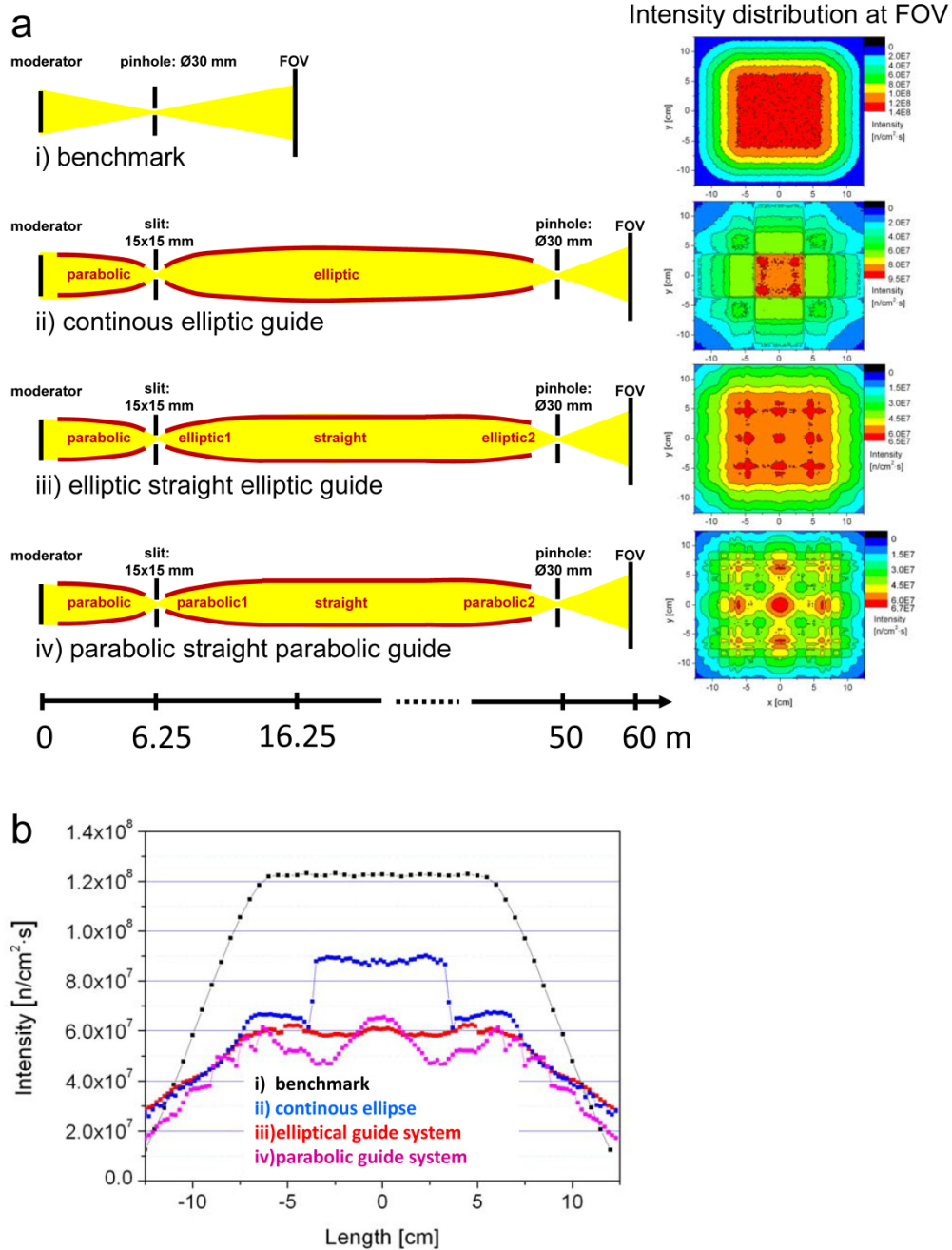


Fig. 1. (a) Comparison between different neutron transport configurations and the proposed benchmark arrangement. The beam paths are shown schematic in yellow. (b) Comparison of horizontal intensity line profiles at the detector position (central line) for the different guide arrangements.

**Table 1. Parameters of the guide systems shown in Fig. 1**

Geometry	F1 L1 S1	L S	F2 L2 S2
ii)	0.275m - m 0.017m	42.2 m 0.108m	1.3m - m 0.0365m
iii)	0.226m 10.5m 0.0185m	20.2m 0.0908m	1.1m 11.7m 0.0361m
iv)	0.5m 19.0m 0.0175m	9.8m 0.1093m	1.1m 13.6m 0.0299m

F1 – entrance focal point position; L1 – length of the entrance guide section; S1 – size of the entrance window; L – length of the middle section; S – size of the middle section; F2 – exit focal point position; L2 – length of the exit guide section; S2 – size of the exit window.

#### 4. Prompt pulse suppression

Another important issue for the beamline is the suppression of the intense prompt  $\gamma$  and fast neutron pulse produced by the spallation process. Although the sensitivity of neutron imaging experiments might not be as pronounced as of some of the neutron scattering experiments, imaging also benefits from a background as low as possible. Three options are taken into account for prompt pulse suppression. On the one hand, a T0 chopper can be used to attenuate the prompt pulse and, on the other hand, the neutron guide can be designed in a way that any direct sight of the source from the detector position is avoided by using kinked or bent guides. These three options have been studied with respect to their influence on beam homogeneity and intensity transfer.

##### 4.1 T0 chopper

A T0 chopper is designed such that the beam is blocked by an appropriate amount of absorber material during prompt pulse emission at a position along the guide where the prompt pulse and the shortest desired neutron wavelength used in the experiments are sufficiently separated in time. On the other hand, the chopper is kept as close to the source as possible in order to attenuate the prompt pulse close to the source and thus to prevent any interference with the longest wavelengths of the previous pulse, even when running at a multiple of the source frequency. Taking this into account and assuming that a similar stopping power as for T0 choppers at J-PARC should be sufficient, such a solution would imply a gap in the guide of about half a meter length at a position between 6.5 m and 10 m distance from the moderator. Consequently, the effect of the interruptions of the guide has been simulated for the favoured guide option (iii). The results obtained are provided in Fig. 2.

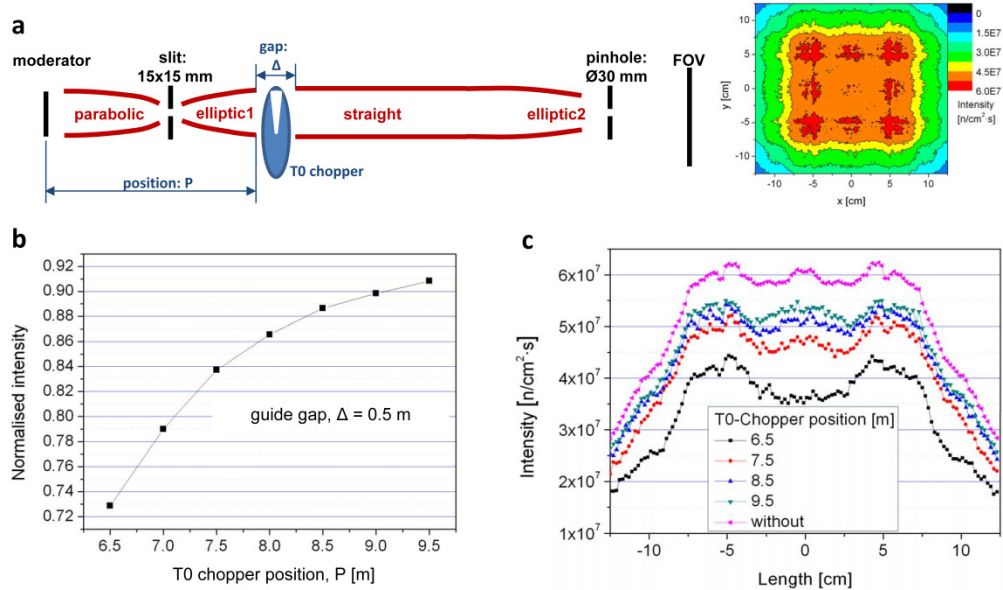


Fig. 2. Influence of chopper position on the intensity gain. (a) The position of the chopper  $P$  was varied with respect to the elliptical guide (elliptic1) which starts at position 6.5 m. The intensity distribution at the detector position (FOV) for a guide gap  $\Delta = 0.5$  m and a favourable chopper position  $P = 8.5$  m are presented in the right-top panel. (b) Transmitted intensity given as a function of the chopper position  $P$ . (c) Intensity line profiles through the centre of the beam at the detector position (FOV) for different positions  $P$ .

The result shows that for a 0.5 m gap at e.g. 8.5 m distance from the source, the intensity drops by 11.4% compared to the configuration without the gap, with no notable change of the intensity profile at the sample position. The increase of intensity with increasing the distance from the moderator can be understood from the fact that the interruption of the guide is located in a diverging region of the elliptical section, and the effect of an interruption becomes less severe the more it is moved to a region of constant guide cross section. On the other hand, a heavy chopper for a larger cross section is a bigger technological challenge than neutron optical solutions. Nevertheless, the 8.5 m and 9 m positions are considered compatible with the current state-of-the-art technology.

#### 4.2 Kinked guide

Another way to avoid background from prompt pulses is to prevent a direct line of sight onto the moderator either by using a guide with a kink or with a curvature. The long straight guide section in the middle of the up to now favoured guide solution (iii) is predestined to be adapted to such an approach. Here the optimization was performed by varying the length of the straight sections and the tilt angle between them in order to achieve maximum intensity at the FOV plane. The parameters for the optimum found are given in Fig. 3.

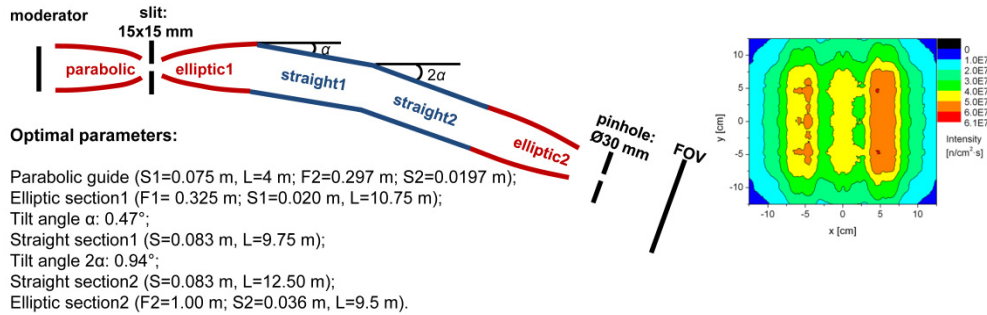


Fig. 3. Proposed kinked guide arrangement for avoiding the direct line of sight onto the moderator. The intensity distribution at the detector position (FOV) for the optimal case is shown on the right.

The arrangement shown in Fig. 3 allows for a deflection of the beam axis by 28 cm at a distance of 60 m from the moderator (FOV plane).

#### 4.3 Bender

The direct line of sight can also be avoided by a bent guide section which turns the beam around an angle in the horizontal plane. In order to keep the bender as short as possible a multi-channel design can be used. In this case, very thin plates covered by supermirror coating are inserted into the guide cavity at equal spacing. The whole package follows the curvature of the bender. The optimization of this arrangement was performed by varying the curvature and the length of the bender which required the use of different number of channels. For the range of distances used in the simulations between 3 and 7 channels were sufficient for closing the direct line of sight. The walls of the channels were 1 mm thick and they were coated by a supermirror coating with  $m = 5$ . The optimal parameters for this configuration including bender with 4 channels are given in Fig. 4.

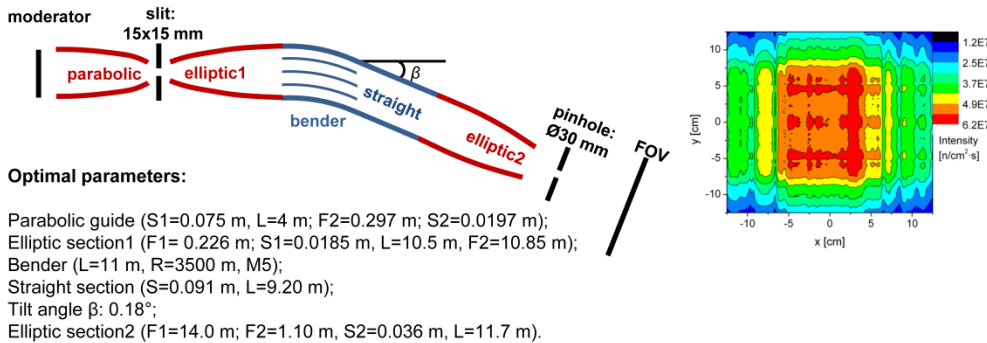


Fig. 4. Proposed bender arrangement for avoiding the direct line of sight onto the moderator. The intensity distribution at the detector position (FOV) for the best case is shown on the right.

The arrangement shown in Fig. 4 allows for a deflection of the beam axis by 13 cm at a distance of 60 m from the moderator (FOV plane). The beam shift here is smaller than for the kinked guide but as can be seen from Fig. 3 the large beam deflection introduces strong beam heterogeneities. Therefore, the bender parameters were set to have the primary beam axis just outside the FOV region.

#### 4.4 Intensity losses and homogeneity

The efficiency of neutron transport through the three different prompt pulse suppression arrangements was monitored by plotting the intensity line profiles across the FOV. A direct

comparison of the profiles for the three cases in combination with the favourable arrangement shown in Fig. 1(aiii) was performed. The comparison of the mean intensity in the plateau region presented in Fig. 5 shows that the different pulse suppression measures lead to the following intensity losses (measured in the plateau): 5% for the T0 chopper (no beam deflection), 5% for the bender as well (13 cm beam deflection), and 20% for the kinked guide arrangement (28 cm beam deflection). Of course the largest beam deflection in case of the kinked guide is the reason for the lower neutron transmission but it should be pointed out that the configurations presented above are optimal solutions for an imaging instrument imposing the criterion of a beam distribution as homogenous as possible combined with the highest transported intensity. Changing the order of priorities of the criteria, e.g. by reversing the order, will lead to different configuration parameters with different performances. The intensity plots in Figs. 2–4 and the profiles in Fig. 5 also yield information about the beam homogeneity at the detector position, which is a very important parameter for any imaging instrument. The T0-chopper configuration provides a beam homogeneity which is very close to the one observed in the favourable straight elliptic arrangement Fig. 1(aiii). The bender configuration provides similar high neutron flux at the sample position as the T0-chopper configuration but with less homogeneity of the beam in the plateau area.

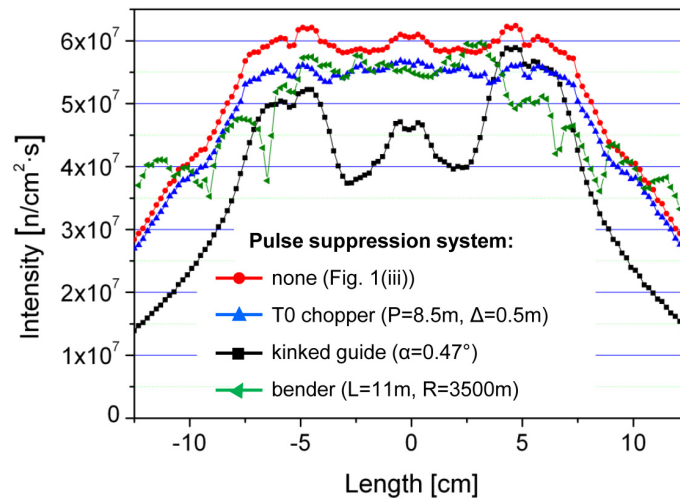


Fig. 5. Comparison of the intensity line profiles for different prompt pulse suppression arrangements used together with the straight elliptic guide system described in Fig. 1(aiii).

#### 4.5 Spectral effects

Due to the importance of spectral homogeneity, especially for conventional white beam imaging experiments and in particular for quantitative data analysis, the spectral homogeneity across the FOV was investigated. In the Monte Carlo simulations a limited wavelength band between 0.5 Å and 7.5 Å was used in order to achieve an efficient computation procedure. For the optimum guide solution (Fig. 1(aiii)), Fig. 6(a) shows simulated spectra in areas of  $20 \times 20 \text{ mm}^2$  at different locations in the FOV from the centre to the edge. Spectral homogeneity is found across the FOV for wavelengths above 2 Å. However, deviations of several per cent have to be taken into account for wavelengths below 2 Å. Moreover, heterogeneities over the moderator surface, which are not yet accounted for, might have to be considered later as well. In the case of prompt pulse suppression by a T0 chopper (for a guide gap  $\Delta = 0.5 \text{ m}$  and a favourable chopper position  $P = 8.5 \text{ m}$ ) as given in Fig. 2 the spectral distribution shows similar spectra as in Fig. 6(a).

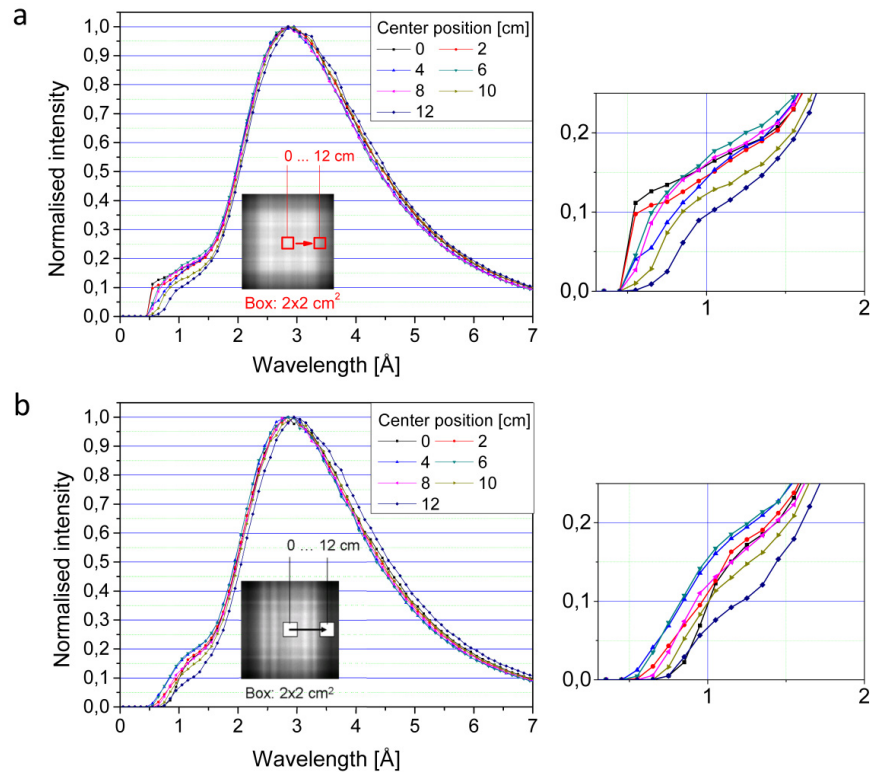


Fig. 6. Spectral distributions at the detector position (FOV) at 60 m distance from the moderator for different lateral displacements from the beam axis for (a) a straight elliptic guide arrangement (Fig. 1(a)) and (b) a kinked guide system (Fig. 3). Enlargements of the plots are shown at the right.

The case of a kinked neutron guide (Fig. 3) was studied as well. The spectral distribution at various locations across the FOV is presented in Fig. 6(b). Similar to the straight guide configuration (Fig. 6(a)) the result shows that the kink influences the spectral distribution as well in the range between 0.5 Å and 1.5 Å where fewer neutrons are transported to the sample position 60 m from the moderator. The second case of beam deflection by using a bender (presented in Fig. 4) shows similar spectral behaviour as seen in Fig. 6(b).

## 5. Conclusions

The neutron guide system of a planned imaging instrument at the long-pulse spallation source ESS was optimised with respect to the maximum of intensity transported to the sample position, the best possible beam homogeneity and least possible spectral distortions. Additional analysis for minimizing the background at the sample position created by prompt pulses was performed. The optimization shows that a combination of a parabolically shaped feeder and an elliptic neutron guide system provides the best combination of beam intensity and homogeneity at the sample position. This is an important design feature with respect to a broad range of instruments in particular at long pulse spallation source, which require a high resolution pulse shaping chopper. As no moving parts such as choppers can be placed in the biological shielding of the source monolith, such geometry referred to as an eye-of-the-needle is to be exploited. Application of a T0 chopper to intercept fast neutrons arriving directly from the moderator is superior to the use of a kinked guide or a bender due to the better spatial characteristics and relatively higher intensity of the transported beam. In particular the required transport of thermal neutrons, i.e. wavelengths shorter than 2 Å, like widely used in

thermal chopper spectrometers and diffractometers, profits from avoiding a directional change in the neutron transport. Additionally, also the study of the position dependence of a guide interruption in the diverging part of a neutron transport system is valuable for a broad range of applications and not only T0 chopper installations.

The next step in the design of the neutron imaging instrument at ESS is the optimization of the chopper arrangement and its adjustment to the already optimized guide system. The contributions of the guide interruptions and imperfections due to joints of the different segments and their misalignments should be investigated additionally where a new run of optimization should be performed when the two major components (guide and chopper systems) are merged together.

The present study showed the complicity of the optimization of neutron guide system for instrumentation at neutron spallation sources and provided some solutions which can be used in the design of future instruments.

### **Acknowledgments**

This work was funded by the German BMBF under “Mitwirkung der Zentren der Helmholtz Gemeinschaft und der Technischen Universität München an der Design-Update Phase der ESS, Förderkennzeichen 05E10CB1”.